(Preprint) AAS 19-053

FAST ATTITUDE MANEUVERS FOR THE LUNAR RECONNAISSANCE ORIBTER

Mark Karpenko,[*] Travis Lippman,[†] I. Michael Ross,[‡] Julie K. Halverson,[§] Timothy McClanahan,[**] Michael Barker,[††] Erwan Mazarico,[‡‡] Rebecca Besser,[§§] Cornelius J. Dennehy,[***] Tannen VanZwieten,[†††] and Aron Wolf[‡‡‡]

This paper describes a new operational capability for fast attitude maneuvering that is being developed for the Lunar Reconnaissance Orbiter (LRO). The LRO hosts seven scientific instruments. For some instruments, it is necessary to perform large off-nadir slews to collect scientific data. The accessibility of off-nadir science targets has been limited by slew rates and/or occultation, thermal and power constraints along the standard slew path. The new fast maneuver (FastMan) algorithm employs a slew path that autonomously avoids constraint violations while simultaneously minimizing the slew time. The FastMan algorithm will open regions of observation that were not previously feasible and improve the overall science return for LRO's extended mission. The design of an example fast maneuver for LRO's Lunar Orbiter Laser Altimeter that reduces the slew time by nearly 40% is presented. Pre-flight, ground-test, end-to-end tests are also presented to demonstrate the readiness of FastMan. This pioneering work is extensible and has potential to improve the science data collection return of other NASA spacecraft, especially those observatories in extended mission phases where new applications are proposed to expand their utility.

INTRODUCTION

The first minimum time attitude maneuver was flown on NASA's Transition Region and Coronal Explorer (TRACE) in August 2010 [1, 2]. In contrast to a standard slew, a minimum time

[*] Research Associate Professor, Dept. Mechanical and Aerospace Engineering, Naval Postgraduate School, Monterey, CA 93943. Corresponding author e-mail: mkarpenk@nps.edu
[†] MS Student, Dept. Mechanical and Aerospace Engineering, Naval Postgraduate School, Monterey, CA 93943.
[‡‡] Distinguished Professor, Dept. Mechanical and Aerospace Engineering, Naval Postgraduate School, Monterey, CA 93943.
[§] Systems Engineer, Space Science Mission Operations, NASA Goddard Space Flight Center, Greenbelt, MD 20771.
[**] Planetary and Computer Scientist, Solar System Exploration Division, NASA Goddard Space Flight Center, Greenbelt, MD 20771.
†† Research Scientist, Planetary Studies, NASA Goddard Space Flight Center, Greenbelt, MD 20771.
‡‡ Research Scientist, Planetary Studies, NASA Goddard Space Flight Center, Greenbelt, MD 20771.
[§§] Systems Engineer, KBRWyle Government Services, Huntsville, AL, 35806.
[***] NASA Technical Fellow, Guidance, Navigation and Control, Goddard Space Flight Center, Greenbelt, MD 20771.
[†††] NASA Engineering and Safety Center, John F. Kennedy Space Center, Kennedy Space Center, FL 32899.
[‡‡‡] Principal Engineer, Guidance and Control Section, Jet Propulsion Laboratory, Pasadena, CA 91109.

attitude maneuver is a non-standard slew that exploits the spacecraft's instantaneous preferred axes of rotation. That is, the minimum-time ('fast') maneuver follows a path that maximizes the momentum-to-inertia ratio as the spacecraft is reoriented to the target attitude. A standard attitude maneuver about the vehicle's roll axis is shown in Figure 1a. The fast maneuver shown in Figure 1b has the same starting and ending attitudes but is accomplished in less time, because it steers the spacecraft motion along the preferred path of greatest agility rather than about the eigenaxis. Typical slew time reductions observed on the TRACE spacecraft were greater than 20% but reduction in slew time ultimately depends on the details of a specific spacecraft's mass properties and attitude control authority. For instance, in some cases, it is possible to generate reduction in slew times in excess of 70%. [10]. A simple procedure for estimating the benefit of implementing a fast maneuver in comparison with a standard slew is based on the spacecraft agilitoid* and is detailed in [3].

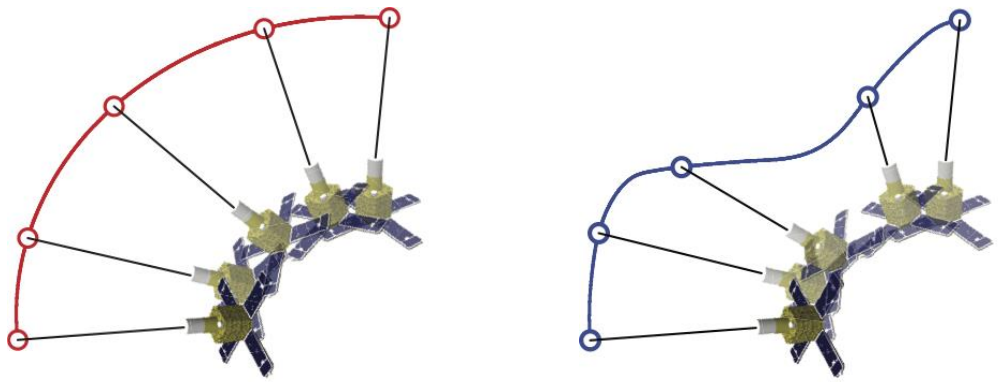

(a) **(b)**

Figure 1. "Snapshots" of TRACE's standard (a) and minimum-time (b) maneuvers reconstructed from telemetry data of the 2010 flight demonstrations.

This paper presents new details related to the recent development of fast attitude maneuvering for NASA's Lunar Reconnaissance Orbiter (LRO). The LRO was launched in 2009 as a robotic mission for mapping the moon's surface. The mission has been extended with a unique set of science objectives aimed at improving our understanding of processes throughout the solar system. The LRO hosts seven scientific instruments. As part of the extended mission operations, it has become necessary to frequently slew through large angles to acquire off nadir science targets. This has pushed the limits of the attitude control system, which was originally designed to support a primarily nadir pointing mission. Using the existing attitude control logic for extended mission science has limited the accessibility of off nadir science targets due to restrictions on slew rates and/or violations of occultation, thermal or power constraints along the standard slew path. The newly developed fast attitude maneuvering algorithm (FastMan) employs a slew path that

* The agilitoid defines the achievable slew capability of a satellite about any axis of rotation in terms of the relationship between the slew torque or momentum authority and the spacecraft mass-properties.

specifically avoids constraint violations while minimizing the slew time. LRO's new slew algorithm is therefore an extension of the minimum-time slew previously demonstrated on the TRACE spacecraft. The main hurdles to overcome in extending the minimum-time slew for implementation on LRO have been in the formulation and inclusion of operational path constraints such as occultation and specifying the maneuver boundary conditions consistent with the pointing geometries required to support the extended mission science objectives.

In LRO's fourth extended mission, the FastMan algorithm is poised to open regions of observation that were not previously feasible. This will improve the overall mission science return. In this paper, the latter aspect is demonstrated for an example involving the Lunar Orbiter Laser Altimeter (LOLA), one of LRO's seven scientific instruments. High-fidelity simulations as well as pre-flight check-out activities conducted using mission tools from NASA Goddard Space Flight Center are presented to demonstrate the flight readiness of the new attitude maneuvers.

ENHANCING LRO'S EXTENDED MISSION SCIENCE RETURN

The LRO (see Figure 2) has seven scientific instruments mounted to a nominally (lunar) nadir facing instrument deck. The Cosmic Ray Telescope for the Effects of Radiation (CRaTER) instrument has characterized the lunar radiation environment and allowed scientists to determine potential impacts to astronauts and other life. The Diviner Lunar Radiometer Experiment (DLRE) has identified cold traps and potential ice deposits as well as rough terrain and other landing hazards by measuring surface and subsurface temperatures from orbit. The Lyman-Alpha Mapping Project (LAMP) has searched for surface ice and frost in the polar regions and has provided images of permanently shadowed regions of the lunar surface. The Lunar Exploration Neutron Detector (LEND) has been used to create high-resolution maps of lunar hydrogen distribution and gather information about the neutron component of the lunar radiation environment. The Lunar Reconnaissance Orbiter Camera (LROC) continues to take high-resolution, black-and-white images of the lunar surface. The Miniature Radio Frequency (Mini-RF) is an advanced radar that has been used to image the polar regions and search for water ice. The Lunar Orbiter Laser Altimeter (LOLA) has been used to generate a high-resolution, 3D map of the moon.

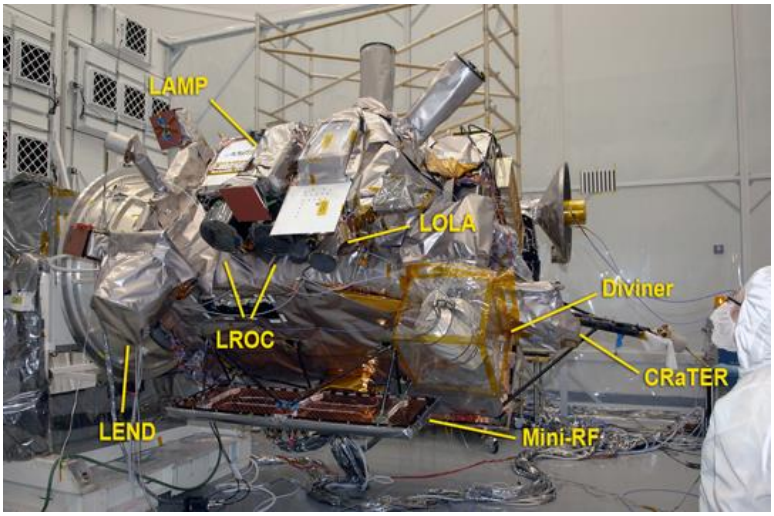

Figure 2. Instrument suite of the Lunar Reconnaissance Orbiter.

In addition to the nadir-facing altimeter, LOLA has a secondary laser ranging (LR) system mounted on the anti-nadir facing high-gain antenna. Normally this ranging system is used to calibrate the primary LOLA instrument. Recently, the LR has been repurposed and used to detect dust near the lunar surface to study Lunar horizon glow. The LR must be slewed to the sunrise or sunset horizon in order to look for evidence of scattered light. This is detected as a rise in signal when the sun is just below the horizon as illustrated in Figure 3.

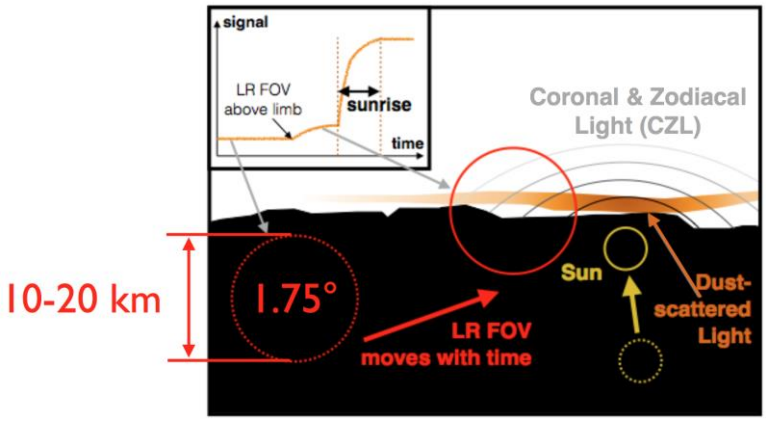

Figure 3. Pointing geometry of LOLA laser ranging sensor for detection of lunar dust.

Because LOLA Lunar horizon glow science typically requires large off-nadir slews to obtain the correct sensor geometries, the ability to collect science has been limited (and at times even prevented) by the time required to do the slews. Therefore, LOLA Lunar horizon glow science activity provides a corner case for evaluating the utility of fast maneuvers for reorienting the LRO.

SPACECRAFT DYNAMICS AND CONTROL

In this section, we present the equations of motion for the LRO spacecraft and describe the observing mode attitude control law that will be used to implement the new fast maneuvers.

Satellite Equations of Motion

The LRO is a three-axis stabilized satellite that uses a set of four reaction wheels with a total momentum storage capacity of 130 Nms for attitude control [5]. The wheels are arranged in a tetrahedron configuration as shown in Figure 4.

The satellite equations of motion may be constructed by assembling the differential equations for the attitude kinematics and the rotational dynamics together with the equations describing the dynamics of the reaction wheel array. The attitude of the satellite is parameterized using a quaternion representation, with the following kinematic differential equation:

$$\dot{\mathbf{q}} = \mathbf{Q}(\omega)\mathbf{q} \tag{1}$$

where

$$\mathbf{Q}(w)=\frac{1}{2}\begin{bmatrix} 0 & w_3 & -w_2 & w_1 \\ -w_3 & 0 & w_1 & w_2 \\ w_2 & -w_1 & 0 & w_3 \\ -w_1 & -w_2 & -w_3 & 0 \end{bmatrix} \tag{2}$$

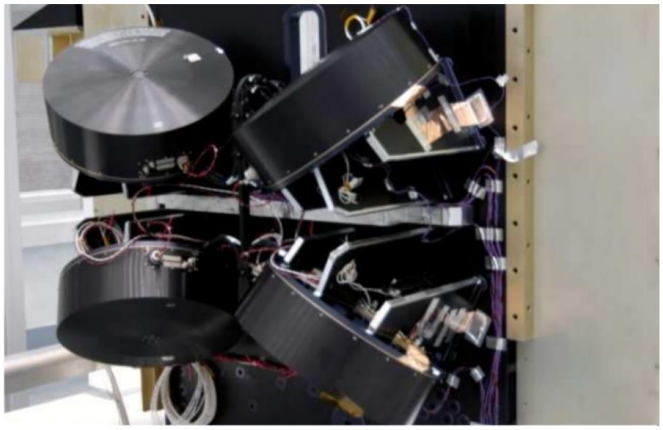

Figure 4. Reaction wheel array on the LRO.

Euler's equations for the rotational dynamics of the satellite are given as [6]

$$\mathbf{I}\dot{\omega}=-\omega\times\left(\mathbf{I}\omega+\mathbf{h}\right)-\tau+\tau_{\text{ext}} \tag{3}$$

where $\mathbf{I}$ is the inertia matrix of the spacecraft. Vector $\mathbf{h}$ is the reaction wheel angular momentum and t is the reaction wheel control torque vector and t_{ext} is the vector of external torques, each expressed in the satellite body-fixed frame.

The reaction wheel angular momenta and the reaction wheel control torques are transformed from the individual wheel spin axes to the body-fixed frame by the following equations

$$\mathbf{h}=I_{\text{w}}\mathbf{Z}\mathsf{W}_{\text{w}} \tag{4}$$

and

$$\tau=\dot{\mathbf{h}}=I_{\text{w}}\mathbf{Z}\dot{\Omega}_{\text{w}}=\mathbf{Z}\tau_{\text{w}} \tag{5}$$

where I_{w} is the inertia of the flywheels and W_{w} is the vector of reaction wheel angular rates. Matrix $\mathbf{Z}$ is a column matrix of unit vectors relating the individual wheel spin axes to the body-fixed frame, i.e. $\mathbf{Z}=[\mathbf{z}_1\,|\,\mathbf{z}_2\,|\,\mathbf{z}_3\,|\,\mathbf{z}_4]$.

Selecting the state vector as $\mathbf{x}=[\mathbf{q}\,|\,w\,|\,\mathsf{W}_{\text{w}}]^T$ and the control vector as $\mathbf{u}=t_{\text{w}}$ give the following state-space model of the satellite dynamics

$$\dot{\mathbf{x}} = \begin{bmatrix} \mathbf{Q}(\omega)\mathbf{q} \\ \mathbf{I}^{-1}\left[-\omega \times (\mathbf{I}\omega + I_{\mathrm{w}}\mathbf{Z}\Omega_{\mathrm{w}}) - \mathbf{Z}\mathbf{u}\right] \\ I_{\mathrm{w}}^{-1}\mathbf{u} \end{bmatrix} \tag{6}$$

Observing Mode Control Law

Slews are implemented using LRO's observing mode attitude control law. Observing mode is used for all nominal pointing and slewing operations including those for science data collection and instrument calibrations [5]. A detailed description of the control law is given in [7] and so only some highlights are given here. The control torque command is determined using a standard PID control law with a proportionally-limited attitude error to generate constant-rate roll, pitch or yaw-axis slews. The control law is given as

$$t_c = \mathbf{I}\left(k_r w_e + k_p \mathrm{proplim}[\mathbf{v}_e] + k_i \grave{\mathbf{O}} \mathbf{v}_e\right) + w' \left(\mathbf{I}w + \mathbf{h}\right) \tag{7}$$

The torque command, t_c, is mapped to the wheels using a pseudoinverse control allocation so that $t_{\mathrm{w}} = \mathbf{Z}^{\#} t_c$, where $\mathbf{Z}^{\#}$ is the Moore-Penrose pseudoinverse of the reaction wheel alignment matrix. In (7), k_p, k_i, and k_r are the PID gains and $\mathbf{v}_e$ is the vector part of the error quaternion given as

$$2\mathbf{q}_e = \begin{bmatrix} \mathbf{v}_e \\ s_e \end{bmatrix} = 2\left[\mathbf{q}_{\mathrm{est}}^{-1} \otimes \mathbf{q}_{\mathrm{tgt}}\right] \tag{8}$$

where $\mathbf{q}_{\mathrm{tgt}}$ is the commanded target quaternion, $\mathbf{q}_{\mathrm{est}}$ is the estimated attitude quaternion and symbol Ä denotes the quaternion multiplication operation. The 'proplim' function in (7) implements proportional limiting on quaternion error for preservation of the attitude vector direction (roll, pitch or yaw) for a rate limited slew. The per-axis rate limit is presently set at 0.13 deg/sec. A third-order elliptic filter, applied to each body axis torque, is used to provide modal suppression of the low frequency spacecraft modes while maintaining adequate linear stability margins [7].

The estimated attitude quaternion, $\mathbf{q}_{\mathrm{est}}$, is derived from a six-state Kalman filter that uses two star trackers and one 3-axis inertial reference unit (IRU) to estimate the IRU bias terms and the spacecraft inertial attitude quaternion. The estimated quaternion is the definitive attitude for onboard attitude control. Due to degradation of LRO's rate gyros, a new zero gyro control mode has been developed that removes the IRU from the Kalman filter and instead uses derived rate data. In this mode, the two star trackers play a dual role and provide the usual attitude reference as well as a derived rate signal that can be filtered to replace the information from the IRU.

PRACTICAL COSIDERATONS

Bright Object/Occultation Constraints

A key challenge in developing a fast attitude maneuver for the LRO is the need to autonomously accommodate practical vehicle attitude, power and thermal constraints. For example, it is necessary to maintain an angle of at least 60-deg between the instrument deck and the Sun. Keep

out constraints also exist for instrument deck Moon and Earth interference, as well as constraints associated with the spacecraft's star trackers. In the zero gyro control mode discussed above, off nadir slews will not be performed if both star trackers are occulted. Satisfaction of these pointing constraints along the maneuver trajectory is critical for operation of the spacecraft.

A schematic for constructing a canonical keep out constraint is given in Figure 5. In Figure 5, unit vector $\hat{\mathbf{b}}^B$ denotes the orientation of an instrument bore-sight with respect to the satellite body-fixed frame. Unit vector $\hat{\mathbf{c}}^N$ denotes the orientation of a bright or occulting body, such as the Sun, Moon or Earth, referenced to an inertial frame, *N*.

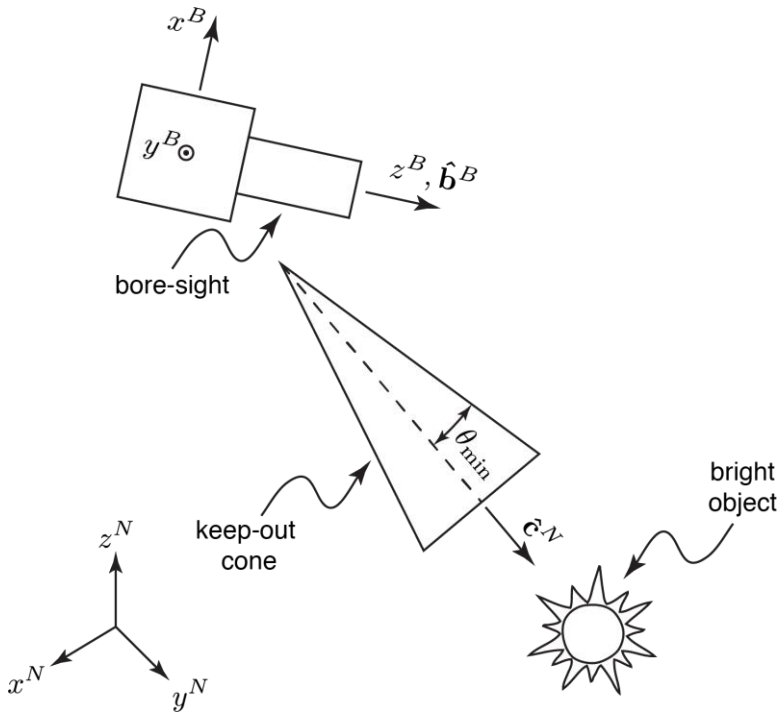

Figure 5. Schematic of bright-object avoidance.

In order to construct an appropriate keep out constraint, it is necessary to express vectors $\hat{\mathbf{b}}^B$ and $\hat{\mathbf{c}}^N$ in the same frame. For example, if it is desired to work in the spacecraft body reference frame, *B*, then the vector pointing to the bright or occulting body must be transformed as $\hat{\mathbf{c}}^B = {}^B\mathbf{C}^N\hat{\mathbf{c}}^N$. On the other hand, if it is desired to work in the inertial reference frame, then the instrument bore-sight vector must be transformed as $\hat{\mathbf{b}}^N = {}^N\mathbf{C}^B\hat{\mathbf{b}}^B$. Thus, the transformation matrix ${}^B\mathbf{C}^N$ is interpreted as a transformation from frame *N* to frame *B* and the transformation matrix ${}^N\mathbf{C}^B$ is interpreted as a transformation from frame *B* to frame *N*.

In order to maintain a target object outside of the bore-sight cone having half-angle $q_{\min}$, as in Figure 5, the following constraint must be satisfied at all times

$$\left[\hat{\mathbf{c}}^B(t)\right]^T\hat{\mathbf{b}}^B \le \cos(q_{\min}) \tag{9}$$

In (9), unit vector $\hat{\mathbf{c}}^B$ is a function of time since the spacecraft is in motion relative to the inertial frame. In the language of dynamic optimization, the keep out constraint is a nonlinear path constraint that must be enforced along any feasible attitude trajectory. Moreover, due to the influence of time on the relative positions of the bodies, the constraint may be binding over an entire maneuver, over only portions of a maneuver, or entirely non-binding.

In order to determine the various $\hat{\mathbf{c}}^B(t) = {}^B\mathbf{C}^N(t)\hat{\mathbf{c}}^N(t)$, planetary ephemeris data referenced to an Earth-Centered Inertial (ECI) frame (J2000) is used. Together with the LRO ephemeris, it is possible to compute the positions and velocities of all the bodies of interest relative to the LRO using the following vector equations in the ECI frame (see also Figure 6):

$$\mathbf{r}^N{}_{\text{M/LRO}}(t) = \mathbf{r}^N{}_{\text{M/E}}(t) - \mathbf{r}^N{}_{\text{LRO/E}}(t) \tag{10}$$

$$\mathbf{r}^N{}_{\text{S/LRO}}(t) = \mathbf{r}^N{}_{\text{S/E}}(t) - \mathbf{r}^N{}_{\text{LRO/E}}(t) \tag{11}$$

$$\mathbf{r}^N{}_{\text{E/LRO}}(t) = -\mathbf{r}^N{}_{\text{LRO/E}}(t) \tag{12}$$

In (10) through (12), the notation 'M/LRO' is taken to mean 'Moon with respect to LRO', etc. The velocities are determined similarly. Next, the transformation matrix ${}^B\mathbf{C}^N$ may be constructed as a sequence of transformations, ${}^B\mathbf{C}^N = {}^B\mathbf{C}^Z\,{}^Z\mathbf{C}^O\,{}^O\mathbf{C}^N$, where frame O is an orbital reference frame and frame Z is a local 'zero-offset' spacecraft reference frame.

The orbital reference frame is defined such that the $+z$-axis points towards the center of the Moon in the orbit plane, the $+y$-axis is in the direction of the normal to the orbit plane and the $+x$-axis completes the right-handed triad. The transformation from the inertial frame to the orbital frame is computed from the ephemeris data as

$${}^O\mathbf{C}^N\left(\hat{\mathbf{r}}_{\text{M/LRO}}, \hat{\mathbf{v}}_{\text{M/LRO}}\right) = \begin{bmatrix} \dfrac{\left(\hat{\mathbf{r}}_{\text{M/LRO}} \times -\hat{\mathbf{v}}_{\text{M/LRO}}\right) \times \hat{\mathbf{r}}_{\text{M/LRO}}}{\left|\left(\hat{\mathbf{r}}_{\text{M/LRO}} \times -\hat{\mathbf{v}}_{\text{M/LRO}}\right) \times \hat{\mathbf{r}}_{\text{M/LRO}}\right|} \\ \dfrac{\hat{\mathbf{r}}_{\text{M/LRO}} \times -\hat{\mathbf{v}}_{\text{M/LRO}}}{\left|\hat{\mathbf{r}}_{\text{M/LRO}} \times -\hat{\mathbf{v}}_{\text{M/LRO}}\right|} \\ \hat{\mathbf{r}}_{\text{M/LRO}} \end{bmatrix} \tag{13}$$

The LRO has two modes of operation that define the local zero-offset reference frame. In the 'forward' mode, the null attitude is such that the spacecraft is aligned with the orbital frame so that ${}^Z\mathbf{C}^O{}_{\text{forward}}$ is the identity matrix. In the 'reverse' mode, the spacecraft is rotated by 180-degrees about the nadir axis. In this case, the transformation to the local zero-offset reference frame is

$${}^Z\mathbf{C}^O{}_{\text{backward}} = \begin{bmatrix} -1 & 0 & 0 \\ 0 & -1 & 0 \\ 0 & 0 & 1 \end{bmatrix} \tag{14}$$

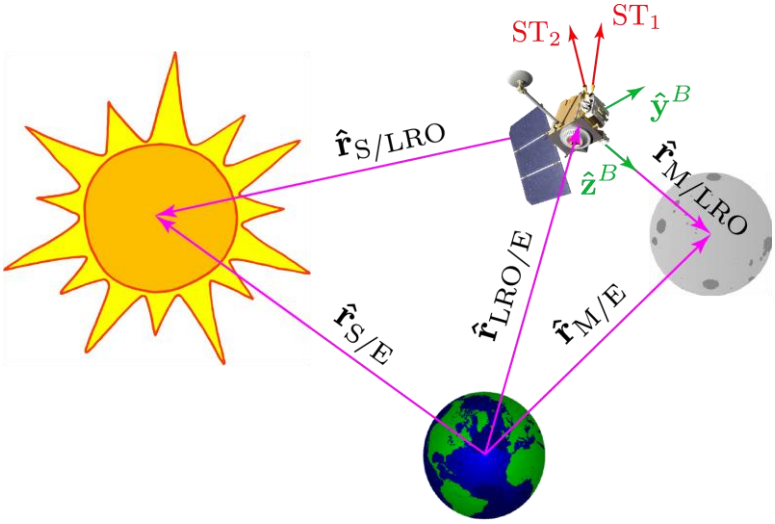

Figure 6. Vectors for computing interference of instrument and sensor bore-sights with bright or occulting objects.

The last transformation, from the local zero-offset frame to the spacecraft body-fixed frame, is defined by the offset quaternion, $\mathbf{q}_{\text{offset}} = [q_1, q_2, q_3, q_4]^T$. The transformation matrix is given by

$$ {}^{B}\mathbf{C}^{Z}\left(\mathbf{q}_{\text{offset}}\right) = \begin{bmatrix} q_1^2 - q_2^2 - q_3^2 + q_4^2 & 2(q_1q_2 + q_3q_4) & 2(q_1q_3 - q_2q_4) \\ 2(q_1q_2 - q_3q_4) & -q_1^2 + q_2^2 - q_3^2 + q_4^2 & 2(q_2q_3 + q_1q_4) \\ 2(q_1q_3 + q_2q_4) & 2(q_2q_3 - q_1q_4) & -q_1^2 - q_2^2 + q_3^2 + q_4^2 \end{bmatrix} \quad (15) $$

The orientations of the star tracker bore-sight vectors are illustrated in Figure 6. For normal operations of the LRO spacecraft, it is necessary to ensure that the star tracker bore-sights do not enter the keep-out cones defined by the angles listed in Table 1. For LRO's new gyroless attitude control mode, at least one star tracker must always remain available or large angle maneuvers will not be performed. In addition to this, it is always necessary to ensure that the instruments (nominally aligned with the +z-axis of the spacecraft) are not pointed to within 63 degrees of the Sun.

Table 1. Minimum interference angles for LRO operation.

Bright Body	Star Tracker 1	Star Tracker 2	+z-body axis
Sun	25 deg	25 deg	63 deg
Moon	15 deg	15 deg	N/A
Earth	15 deg	15 deg	N/A

Operational Boundary Conditions

Boundary conditions for a given maneuver are determined by project scientists to satisfy the requirements for scientific data collection. For LOLA Lunar horizon glow science, this is done

using a specialized set of tools to identify time-tagged sets of desirable sunrise/sunset collection geometries. From these sets, several candidates are selected that can be accommodated in the mission-planning schedule and that do not conflict with other planned science activities. Determining the target attitude for science collection is done by pointing the laser ranging bore-sight slightly off of the Sun vector. The lunar geography is taken into consideration to fine tune the target attitude so that geographical features do not block the instrument field-of-view. LOLA Lunar horizon glow science is conducted using the LRO's offset quaternion mode so that the instrument field-of-view will drift across the horizon during the science collection activity even though the slew is a rest-to-rest maneuver. An example of this bore sight motion is illustrated in Figure 3.

FASTMAN PROBLEM FORMULATION

For the LRO spacecraft, we are interested in determining minimum-time maneuvers with attitude as well as other dynamic and engineering constraints. This objective is achieved autonomously by solving a dynamic optimization problem as part of the ground-based maneuver planning process. The FastMan algorithm is intended to be inserted as a new maneuver planning mode into LRO's existing attitude maneuver (AttMan) planning software [11] to enable a seamless integration of fast maneuvering into the LRO's standard mission planning workflow. In its simplest form, the problem formulation for dynamic optimization can be written as

$$
P:\begin{cases}
\text{Minimize} & J = t_f - t_0 \\
& \dot{\mathbf{x}} = \mathbf{f}(\mathbf{x},\mathbf{u}) \\
& [\mathbf{q}(t_0),\omega(t_0),\Omega(t_0)] = [\mathbf{q}^0,\omega^0,\Omega^0] \\
& [\mathbf{q}(t_f),\omega(t_f),\Omega(t_f)] = [\mathbf{q}^f,\omega^f,\Omega^f] \\
\text{Subject to} & |\omega_i| \le \omega_{\max} \quad \text{for } i = 1,2,3 \\
& |\alpha_j| \le \alpha_{\max} \quad \text{for } j = 1,2,3 \\
& \left[\hat{\mathbf{c}}_k^B(t)\right]^T \hat{\mathbf{b}}_k^B \le \cos(\theta_{\min,k}) \quad \text{for } k = 1,2,\ldots,N \\
& u_{\min} \le u_l \le u_{\max} \quad \text{for } l = 1,2,3,4
\end{cases}
\tag{16}
$$

The fast maneuver problem formulation and its variations are solved using a numerical algorithm to determine the state-control function pair, $t \to (\mathbf{q},w,\mathrm{W},\mathbf{u})$ that allows the satellite to be reoriented between the given boundary conditions in the shortest time. A key element in solving fast maneuvers autonomously lies in proper scaling and balancing of the problem equations (see [8, 9]). As part of the solution process, constraints on the spacecraft angular rate, acceleration and reaction wheel control torque are enforced, as are the $N = 9$ interference constraints. In other formulations of the fast maneuver problem, additional operational constraints such as thermal or power and/or details pertaining to the attitude control system dynamics are included as necessary in order to obtain flight ready solutions.

Example Fast Maneuver

To illustrate the application of the FastMan algorithm, a fast maneuver was developed for performing horizon glow science with the LOLA instrument. The slew was designed as an alternative maneuver to support a planned collection activity scheduled for November 17, 2017. This maneuver will hereafter be referred to as the 'day-321' maneuver. The day-321 maneuver was developed as part of a shadowing exercise where fast maneuver profiles were designed in parallel with the conventional planning process in order to test the new ground workflow.

The requirements for the day-321 slew were to perform a rest-to-rest maneuver to the science objective such that the bore-sight of LOLA's secondary laser ranging (LR) system was aligned with a pre-determined location on the Lunar horizon at 03:25:55 UTC. The required quaternion offset from nadir, $\mathbf{q}_{\text{tgt}} = [-0.803, 0.150, -0.226, 0.531]^T$, was determined by the LOLA project scientists. The fast maneuver trajectory obtained by solving (16) is shown in Figure 7. For this fast maneuver, the interference constraints were non-binding. Figure 7a shows the offset attitude quaternions for the maneuver. In a conventional maneuver, the quaternions increase or decrease monotonically towards their desired values. This is because in a conventional maneuver the spacecraft rotation is constrained to occur about the eigenaxis, for example, the roll, pitch, or yaw axis. In a fast maneuver, however, small off-eigenaxis motions are inserted in order to capitalize on the physics of rigid body motion. This allows the satellite to move advantageously about axes that are the least restrictive to rotational motion. As a consequence, the fast maneuver builds up rate about all three body axes simultaneously (see Figure 7b) and utilizes the reaction wheels to modulate the off-eigenaxis rotations in a way that ensures the desired attitude quaternion is achieved at the end of the maneuver.

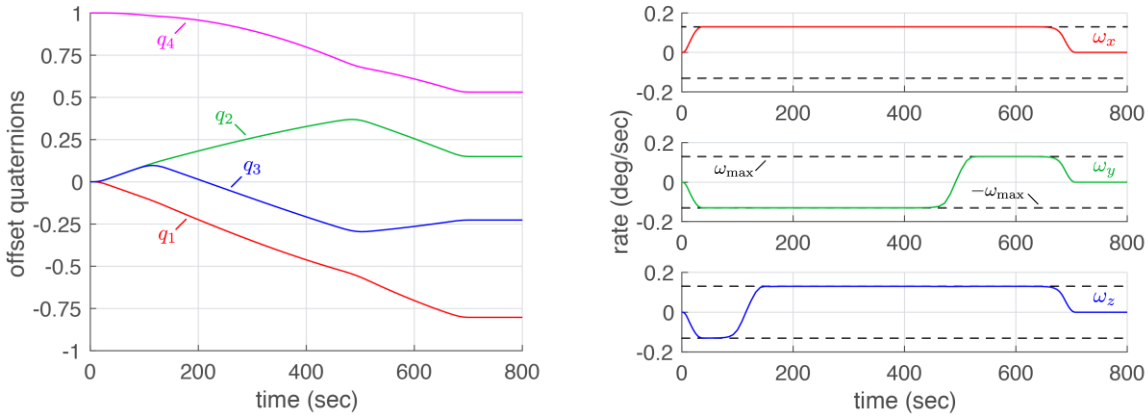

(a) **(b)**

Figure 7. Example fast maneuver to support a LOLA Lunar horizon glow science opportunity on November 17, 2017: (a) offset attitude quaternions; (b) spacecraft body-rates.

To illustrate the utility of fast maneuvering over the existing maneuver plan, the fast maneuver trajectory of Figure 7a can be mapped to inertial quaternions for comparison against the standard slew. A plan using the FastMan algorithm and a standard attitude maneuver plan were both constructed for the day-321 LOLA science collection activity. Each plan included a maneuver from a nadir-pointing attitude out to the science attitude followed by a 10-minute collection window during which the data pertaining to the horizon glow experiment should be collected. Then, a second

maneuver was planned to return the satellite from the science attitude back to nadir pointing. The two maneuver plans are shown in Figure 8.

Referring to Figure 8, the time for the day-321 LOLA science maneuver is reduced by approximately 38% and the total time footprint for the science activity was compressed from 43.6-minutes to 33.6 minutes using the FastMan algorithm. There are two ways that this time savings can be leveraged by the LRO mission. First, all off-nadir science activities must be completed within a 60-minute window. This time period includes the maneuver to the science objective, the collection activity itself and the return maneuver. Thus, the reduction in slew time allows the LOLA instrument to collect additional data within the allotted 60-minute window if this is desired. The new fast maneuvering capability can therefore be advantageous when long off-nadir collection windows are required. Second, it may be the case that the required science activity can be fully completed without violating the 60-minute off-nadir time limit. In this situation, fast maneuvering still reduces the total off-nadir time duration. This frees up time in the mission plan for other instruments to perform tasks. In addition, fast maneuvering has also been identified as an enabling capability for use during periods of eclipse, when opportunities for science observations requiring large slews are often missed because the long time-durations required with the solar panels pointed off-sun cause violations of power or thermal constraints.

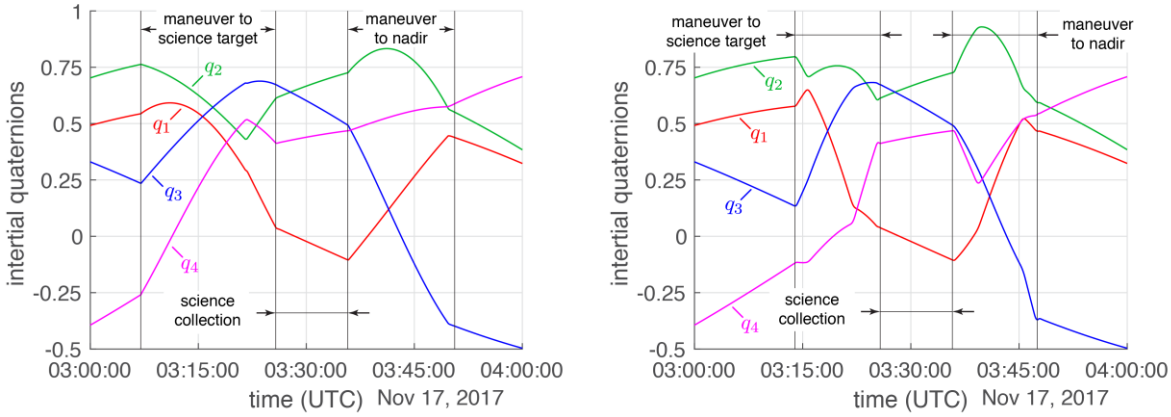

(a) **(b)**

Figure 8. Maneuvers plans for LOLA science activity on November 17, 2017: (a) standard maneuver plan; (b) maneuver plan obtained using FastMan algorithm reduces maneuver time by nearly 40%.

MANEUVER PLANNING AND PRE-FLIGHT VERIFICATION

In this section, we show how FastMan can integrate into the workflow for LRO attitude maneuver planning and describe some of the various checks that are done to validate a maneuver plan prior to flight. Figure 9 shows a simplified schematic of the attitude maneuver planning process that is performed as part of the LRO ground support segment as NASA GSFC. The attitude maneuver planning tool for LRO is the `AttMan` utility [11]. `AttMan` generates a sequence of attitudes for all maneuvers requested by the mission operations center which, in turn, receives maneuver requests from the individual project scientists in the form slew requests. As part of the attitude maneuver planning process, `AttMan` performs checks on pointing constraints and outputs times, attitudes and commanding keywords in the form of a slew plan that can be ingested by

ground support software to create operational (ops) products. The ops products are a collection of data files that are ultimately utilized to generate the command and control sequences that are uplinked and stored on the spacecraft for real-time execution. `AttMan` also produces a predicted attitude file that is used for downstream constraint and operational checks on the output maneuver plan. The new `FastMan` algorithm has been developed as a 'plug-in' module that can be accessed by the `AttMan` utility (see Figure 9) via new slew request keywords in order to generate a fast maneuver profile as described in the previous sections.

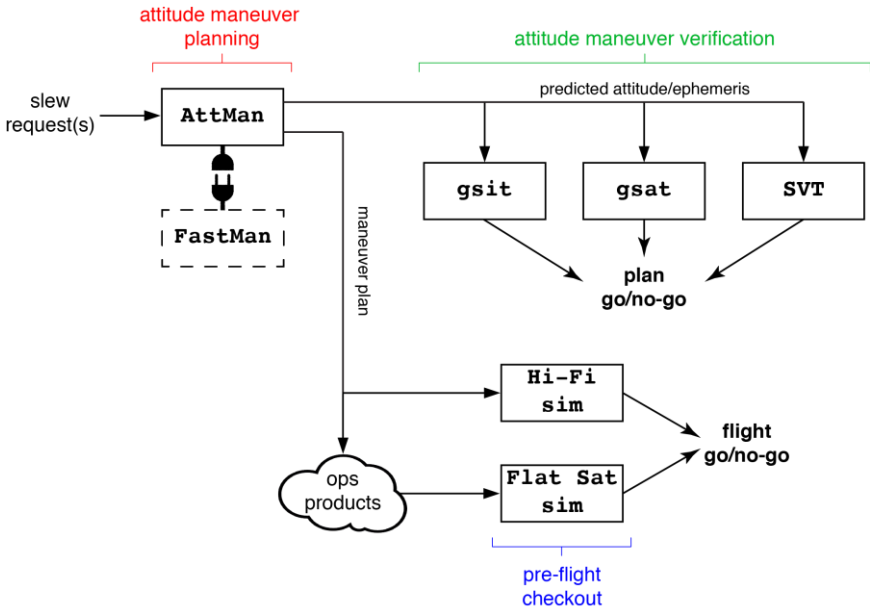

Figure 9. Attitude maneuver planning workflow.

Referring to Figure 9, attitude maneuver verification is done using a series of utilities developed to check various operational constraints. The general sensor interference tool (`gsit`) is a utility used to check a maneuver plan for star tracker interference and to validate that the +z-axis Sun angle constraint is not violated. An example output for LOLA's fast maneuver is shown in Figure 10. During the fast maneuver to the science objective, the Sun is visible to the scientific instruments (+z-axis). However, since the objective of the science activity is to point LOLA's LR in the direction of the Sun, the angle between the Sun and the +z-axis will be increased well above the constraint (denoted in Figure 10 as the value of $q_{\min}$). This is because the LR is mounted on the spacecraft's high-gain antenna, which points in the –z direction. The +z-axis will therefore be pointed away from the Sun. During the science collection activity, the Sun is occulted by the Moon because the Sun has set over the Lunar horizon. During the occultation by the Moon there is no restriction on the Sun angle and so the Sun angle for the maneuver back to the nadir pointing orientation can be less than the $q_{\min}$ threshold as shown in Figure 10. Once back in the nadir pointing orientation, the Sun angle increases with time and is above the $q_{\min}$ threshold when the Sun again becomes visible to the scientific instruments.

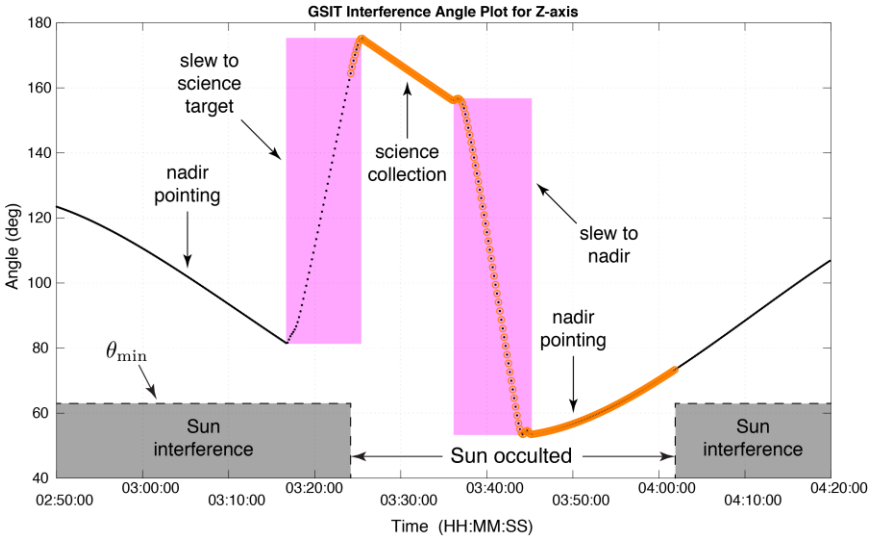

Figure 10. Verification of Sun interference angle for FastMan using `gsit`.

The guide star analysis tool (`gsat`) is utilized to visualize the motion and orientation of the LR bore-sight for Lunar horizon glow science. The output of `gsat` is shown in Figure 11a for LOLA's fast maneuver. As is seen, the LR sensor field-of-view is oriented at the Lunar horizon just after the Sun has set. In the `gsat` output, the Moon has been made slightly transparent so that the position of the Sun relative to the sensor field-of-view can be observed. As shown Figure 11, the Sun is located just beneath the horizon line when the sensor arrives on target. A similar visualization (Figure 11b) has been done to illustrate the actual orientation of the sensor during the science collection activity. Comparing Figures 11a and 11b, it is observed that the on-target bore-sight direction for LOLA's fast maneuver is the same as the bore-sight direction obtained from telemetry. In addition to confirming the sensor orientation during the science collection window, the `gsat` tool can also be used to visualize the movement of the LRO during the fast maneuver to get a sense of how the rotational motion of the fast maneuver differs from that of the standard slew.

The last tool used for verification of attitude maneuver plans is the slew verification tool (`SVT`). `SVT` is primarily used to check thermal and power constraints. This is done by computing various angles and tracking their changes during maneuvering. `SVT` will be used to verify fast maneuvers by checking these angles. `SVT` continues to be updated with more detailed models of the battery charge/dis-charge states. While this effort is primarily aimed at supporting better decision making for mission planners – particularly for activities scheduled during low-beta periods – the updated power models can be inserted into the FastMan algorithm to enhance maneuver design.

There are two pre-flight checkout tools available to verify maneuvers prior to their implementation on orbit. The first tool is the LRO high-fidelity simulation (`Hi-Fi sim`) that implements a model of the spacecraft and its attitude control system in MATLAB/Simulink. `Hi-Fi sim` is used primarily for engineering support and development activities. For example, `Hi-Fi sim` played a key role in the design and testing of LRO's new gyroless attitude control mode. `Hi-Fi sim` is also the tool used to validate the flight-readiness of the FastMan concept and for development and testing of a new spacecraft commanding scheme for operational implementation of the FastMan attitude profiles.

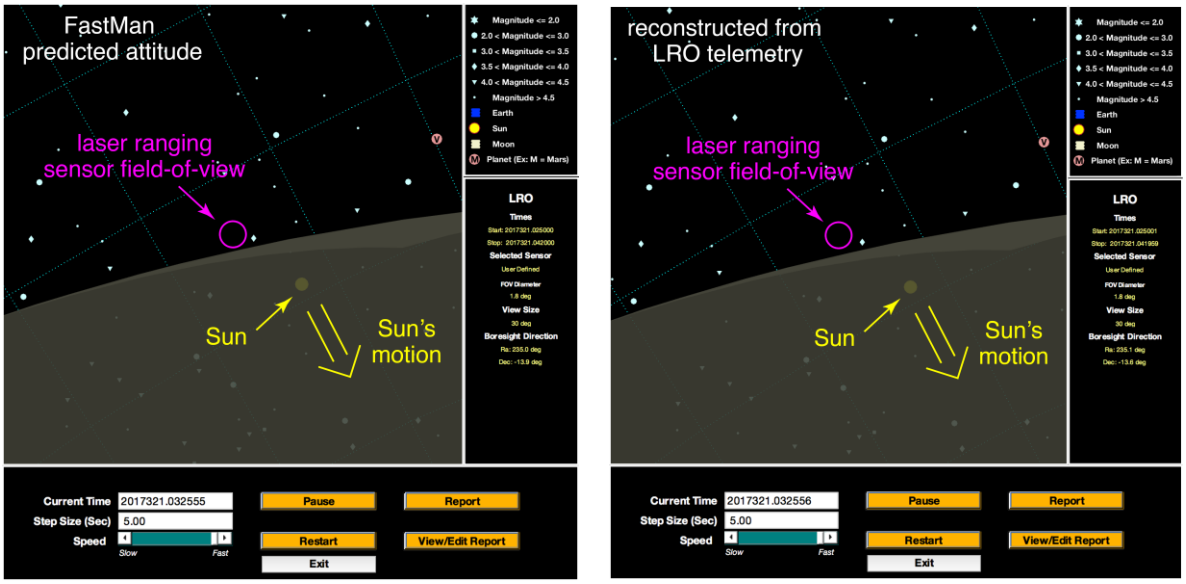

(a) **(b)**

Figure 11. Screenshots of `gsat` output showing the on-target laser ranging sensor bore-sight orientation for a Lunar horizon glow science opportunity on November 17, 2017: (a) bore-sight orientation obtained from FastMan predicted attitude; (b) actual bore-sight orientation obtained from spacecraft telemetry.

Example `Hi-Fi sim` output for LOLA's day-321 fast maneuver is shown in Figure 12. The maneuver was implemented by utilizing LRO's existing quaternion error feedback system to track the FastMan attitude profiles. The attitude profiles will be reproduced on the vehicle by utilizing an interpolation filter. This reduces the rate at which commands need to be read from the spacecraft command storage buffer to reduce uplink and data storage requirements on the spacecraft. Further details on this innovation can be found in reference [12].

Figure 12a shows that the actual attitude quaternions lag the commands somewhat. This is a result of the fact that the spacecraft attitude control system was not designed as an input tracking system but rather simply to regulate to attitude setpoints. This does not present a practical challenge, however, because the time constant of the attitude control is quite small in comparison with the overall maneuver time. The spacecraft angular rates are shown in Figure 12b. The plots show that the attitude control system can implement the fast maneuver while properly adhering to the specified attitude rate limits. This is possible because these rate limits were considered explicitly in the fast maneuver design by the FastMan algorithm.

In contrast to `Hi-Fi sim`, the flat-sat simulator (`Flat Sat sim`) implements a hardware-in-the-loop simulation of LRO's flight computer. Thus, operation of the `Flat Sat sim` for fast maneuvering verifies that the `FastMan` plug-in and its associated ground workflow can correctly generate all of the relevant ops products that must be ingested by the spacecraft for flight. In addition, `Flat Sat sim` will be used to vet any flight software patches that are needed to fully integrate FastMan before they are uplinked to the spacecraft. Some preliminary testing of `FastMan` has been successfully completed using `Flat Sat sim`, and an engineering flight test plan for incorporating FastMan into LRO day-to-day operations has been developed and will be executed at NASA GSFC.

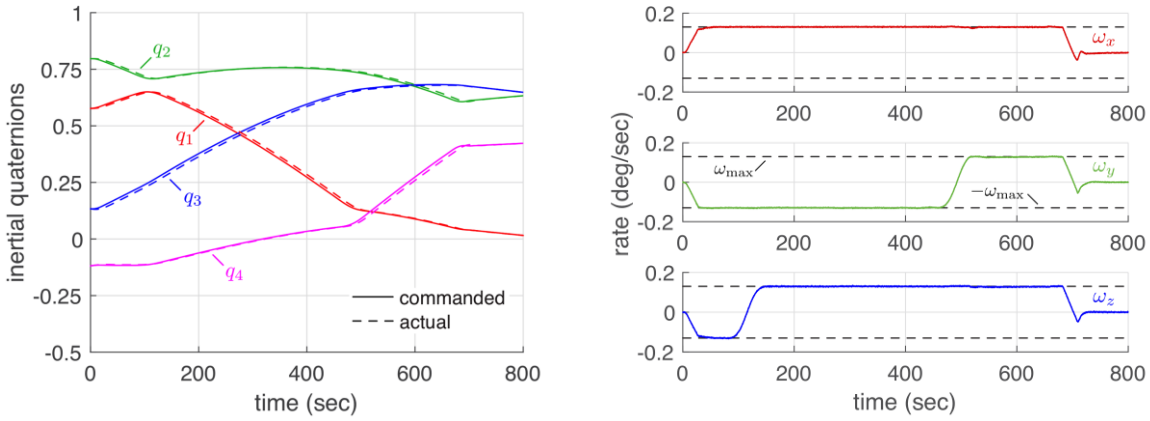

(a) **(b)**

Figure 12. `Hi-Fi sim` of FastMan for a Lunar horizon glow science opportunity on November 17, 2017: (a) inertial attitude quaternions; (b) spacecraft angular rates in body frame.

SUMMARY

The demands of extended mission science operations often push a spacecraft's attitude control systems to its limits. This is because achieving extended mission objectives can require utilization of the scientific instruments in ways that were not conceived as part of the original attitude control design. This paper described an algorithm for faster maneuvering that was tailored for use NASA's Lunar Reconnaissance Orbiter (LRO). Analysis shows that the FastMan algorithm will open regions of observation that were not previously feasible in LRO's third extended mission. The paper includes an example of the design of a fast maneuver for LRO's Lunar Orbiter Laser Altimeter. For this science activity, slew time is reduced by nearly 40%. End-to-end pre-flight and ground-tests were also presented to demonstrate the readiness of FastMan for its planned insertion into the day-to-day operation of the LRO. This pioneering work is extensible beyond LRO and has potential to improve the science data collection return capability of other spacecraft, especially observatories in their extended mission phases looking to expand their utility by pursuing new, unplanned applications.

REFERENCES

[1] Karpenko, M., Bhatt, S., Bedrossian, N., Fleming, A., and Ross. I. M., "First Flight Results on Time-Optimal Spacecraft Slews," *Journal of Guidance Control and Dynamics*, 35(2), pp. 367-376, 2012.

[2] Karpenko, M., Bhatt, S., Bedrossian, N., and Ross, I. M., "Flight Implementation of Shortest-Time Maneuvers for Imaging Satellites," *Journal of Guidance, Control, and Dynamics*, 37(4), pp. 1069-1079, 2014.

[3] King, J. T. and Karpenko, M., "A Simple Approach for Predicting Time-Optimal Slew Capability," *Acta Astronautica*, Vol. 120, pp. 159-170, 2016.

[4] Markley, F. L. and Crassidis, J. L., Fundamentals of Spacecraft Attitude Determination and Control, Springer, New York, 2014.

[5] Shah, N., Calhoun, P., Garrick, J., Hsu, O., and Simpson, J., "Launch and Commissioning of the Lunar Reconnaissance Orbiter," Paper Number: AAS 10-085.

[6] Sidi, M. J., *Spacecraft Dynamics and Control: A Practical Engineering Approach*, Cambridge University Press, New York, 2000.

[7] Calhoun, P. C., and Garrick, J. C., "Observing Mode Attitude Controller for the Lunar Reconnaissance Orbiter," *20th International Symposium on Space Flight Dynamics*, Annapolis, MD, September 24-28, 2007.

[8] Lippman, T., Kaufman, J. M., and Karpenko, M., "Autonomous Planning of Constrained Spacecraft Reorientation Maneuvers," *AAS/AIAA Astrodynamics Specialist Conference*, August 20 - 24, 2017 Stevenson, WA. Paper number: AAS 17-676.

[9] Ross, I. M., Gong, Q., Karpenko, M., and Proulx, R. J., "Scaling and Balancing for High-Performance Computation of Optimal Controls," *Journal of Guidance, Control, and Dynamics*, 41(10), pp. 2086-2097, 2018.

[10] Fleming, A., Sekhavat, P., and Ross, I. M., "Minimum-Time Reorientation of a Rigid Body," *Journal of Guidance, Control, and Dynamics*, 33(1), pp. 160-170, 2010.

[11] Sedlak, J. and Houghton, M., "Lunar Reconnaissance Orbiter (LRO) Attitude Maneuver Planning," *Proceedings of the 21st International Symposium on Spaceflight Dynamics*, Toulouse, France, 2009.

[12] Karpenko, M., Halverson, J. K., and Besser, R., "Waypoint Following Dynamics of a Quaternion Error Feedback Attitude Control System,"*AAS/AIAA Spaceflight Mechanics Meeting*, January 13 - 17, 2019 Ka'anapali, HI. Paper number: AAS 19-283.